Polymer Journal (2022) 54:335–343
https://doi.org/10.1038/s41428-021-00583-y

ORIGINAL ARTICLE

Tuning the thermal and mechanical properties of poly(vinyl alcohol) with 2,5-furandicarboxylic acid acting as a biobased crosslinking agent

Nam Vu Trung[1] · Ni Pham Thi[1] · Thu Ha Nguyen[1] · Mai Ngoc Nguyen[1] · Dung Tran Anh[1] · Thanh Nguyen Trung[1] · Tung Tran Quang[1] · Hau Than Van[1] · Thuy Tran Thi[1]

Received: 7 September 2021 / Revised: 19 October 2021 / Accepted: 21 October 2021 / Published online: 18 November 2021

Abstract

In this study, poly(vinyl alcohol) (PVA) was crosslinked via catalyst-free solid-state esterification at 120 °C with 2,5-furandicarboxylic acid (FDCA) at concentrations ranging from 1 to 10%. The structural characterization of the obtained products was carried out by attenuated total reflection Fourier transform infrared spectroscopy. The effects of ester crosslinks on the water absorption properties of the modified products were investigated through swelling degree analysis. The improvement in thermal properties of the obtained products was confirmed by thermal gravimetric analysis/differential thermal analysis, which showed that thermal stability was optimal for low concentrations of FDCA, i.e., 1 and 5%, where degradation maximums occurred at 354 and 371 °C, respectively, compared to 267 °C for unmodified PVA. The mechanical properties of the products were also studied via tensile testing, where the tensile strength of the crosslinked PVA using 5% FDCA (48.2 ± 2.6 MPa), doubled when compared to untreated PVA (25.5 ± 1.2 MPa).

Introduction

The commercialization of biodegradable polymers and their derived blends or composites is important for achieving a sustainable environment in the near future [1–3]. The utilization of biodegradable products has been a promising approach for addressing plastic pollution and facilitating waste management [2, 4–6], and it encourages the development of clean technologies. An example of biodegradable polymers is poly(vinyl alcohol) (PVA), which has attracted significant attention [7–9]. PVA is a thermoplastic, semi-crystalline, and cost-effective polymer. It is widely commercialized in a variety of applications, such as fabric and paper sizing, fiber coatings, adhesives, emulsion polymerization, packaging, and agricultural films [10, 11]. However, further expansion of PVA applications is restricted by its high level of water absorption. Water acts as a plasticizer, which drastically reduces the mechanical properties of PVA. In addition, the mechanical strength of PVA is relatively low compared to other popular but non-biodegradable synthetic polymers [12–14].

To overcome PVA's high level of water absorption, crosslinking is widely applied. PVA's crosslinked structure can be created by covalent bonds between polymer chains. This process can be influenced based on the choice of crosslinking agents, such as glutaraldehyde [15–18], glyoxal [19], trisodium trimetaphosphate [20], boric acid [21], maleic acid [22], fumaric acid [23], citric acid [12, 24, 25], tartaric acid [26, 27], and succinic acid [28]. Crosslinking has an effect on the water absorption, separation ability and thermal and mechanical properties of PVA. However, in recent literature, there are only a limited number of references regarding the use of aromatic [14, 29, 30] or bioderived crosslinkers [12, 24–27].

A potential crosslinker is 2,5-furandicarboxylic acid (FDCA), a renewable organic compound consisting of two carboxylic acid groups attached to a central furan ring. It is synthesized from 5-hydroxylmethylfurfuran [31–34], a biological precursor that can be synthesized directly from biomass [35–38]. FDCA has recently received a great deal of interest as an alternative to the very common petrochemical monomer terephthalic acid, and it can replace this monomer to synthesize biobased polymers with comparable

✉ Thuy Tran Thi
thuy.tranthi3@hust.edu.vn

[1] Hanoi University of Science and Technology, 1 Dai Co Viet street, 100000 Hanoi, Vietnam

properties [39–42]. The barrier properties of these polymers are even superior to those of their terephthalic acid-based counterparts [43–45]. In addition, because it is a diacid, FDCA can be employed as a crosslinking agent to enhance the properties of PVA. The presence of furan rings in the PVA structure is expected to have a remarkably positive effect on the thermomechanical properties of the product.

Recently, PVA was crosslinked with maleic anhydride (MA) and FDCA under conventional heating and microwave irradiation to obtain different PVA/MA and PVA/FDCA membranes. The optimal crosslinking agent concentration, reaction time, and activation method were examined [30]. However, the thermal and mechanical properties of the product modified by FDCA have not been investigated thoroughly [30].

In this study, the objective was to synthesize and characterize the structure and properties of PVA-crosslink-FDCA materials. The films were prepared by the solution casting method starting from solutions of PVA and FDCA in dimethyl sulfoxide (DMSO). The crosslinking reaction was carried out via catalyst-free solid-state esterification at 120 °C. The formation of ester crosslinks between PVA and FDCA was confirmed by Fourier transform infrared spectroscopy (FTIR). A swelling study was utilized to examine the water absorption of the crosslinked PVAs. Their thermal properties were evaluated using thermogravimetric analysis (TGA). The improvement in the mechanical properties of PVA-crosslink-FDCA films compared to PVA was investigated by tensile measurements.

Experimental procedure

Materials

PVA (CAS: 9002-89-5) (degree of polymerization, 1750 ± 50; degree of hydrolysis, 99%) was purchased from Shanghai Zhanyun Chemical Co., Ltd (China). The hydrolysis degree of PVA was obtained from ^{1}H NMR. FDCA (CAS: 3238-49-2) was provided by Sigma–Aldrich (USA). DMSO (CAS: 67-68-5) was obtained from Merck (Germany). Other chemical products were also purchased from Sigma–Aldrich (USA). All chemicals were used as received.

Methods

As seen in Fig. 1, PVA-crosslink-FDCA films were prepared by solution casting method. The PVA solution (5% w/w) was prepared by dissolving PVA in DMSO at 50 °C for 6 h. The obtained solution was mixed with an FDCA/DMSO solution, and continued to be stirred for 2 h at room temperature. Different acid concentrations (0, 1, 5, and 10% (w/w)) with respect to PVA were used. The solutions were poured into a petri dish and dried for 72 h at 50 °C to obtain PVA films containing dissolved FDCA. The completely dried FDCA/PVA films were crosslinked by heating at 120 °C in an oven for 2 h to obtain the PVA-crosslink-FDCA films. The reaction between PVA and FDCA is displayed in Fig. 2.

These films were then stored in a desiccator at ambient temperature to avoid moisture uptake. Except for the swelling study, all samples were equilibrated at the conditions of 25 °C and 50% relative humidity (RH) before the measurements.

Characterization of films

Fourier transform infrared spectroscopy (FTIR)

Infrared spectra of the samples were recorded on a Nicolet iS50 FTIR (Thermo Fisher Scientific) spectrometer in attenuated total reflection (ATR) mode. The specimens were measured directly with a scan range from 400 to 4000 cm^{-1}.

Swelling study

The swelling behavior of PVA and crosslinked PVA films in deionized water was investigated at 25 °C. The swelling degree (SD) was evaluated by the gravimetric method using the difference between the weights of the dried samples and the equilibrated films in water. First, dry films were cut into 2 cm × 2 cm pieces, weighed and then immersed in deionized water for 24 h. Afterward, the samples were removed from the water, and the remaining water on the surface of the sample was removed before weighing. The SD was calculated using the following equation:

$$SD(\%) = \frac{W_S - W_D}{W_D} \times 100$$

where W_S is the weight of swollen samples and W_D is the weight of dry samples.

Thermal gravimetric analysis (TGA)

The thermal properties of all specimens were analyzed under a nitrogen atmosphere on a Linseis STA PT1600 analyzer. The temperature was increased from 25 to 600 °C, with a heating rate of 10 °C/min.

Tensile testing

The samples in the form of a thin film were cut into a dumbbell shape with dimensions according to ASTM D882. Young's modulus, stress at break, and elongation at break were determined using a Zwick Tensiler Z 2.5 testing

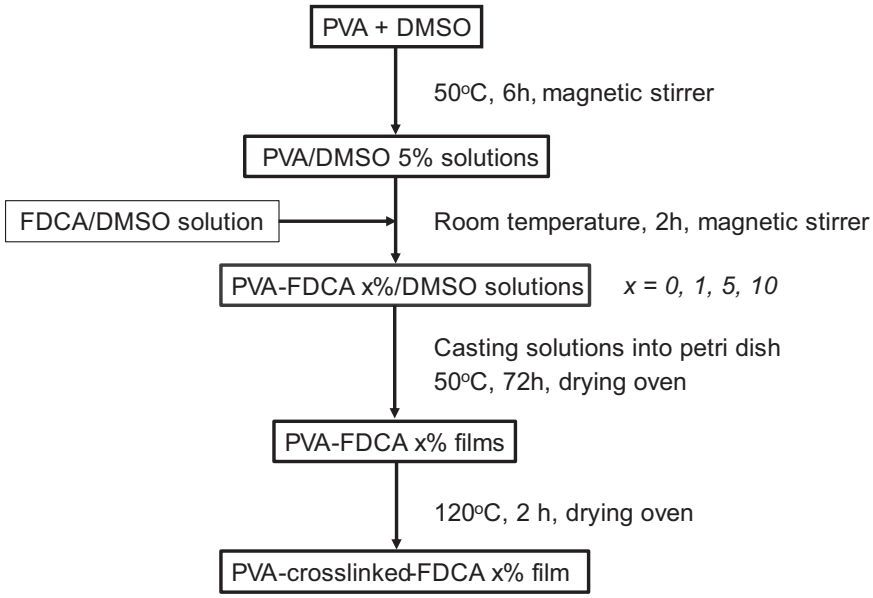

Fig. 1 Schematic overview of PVA-crosslink-FDCA preparation

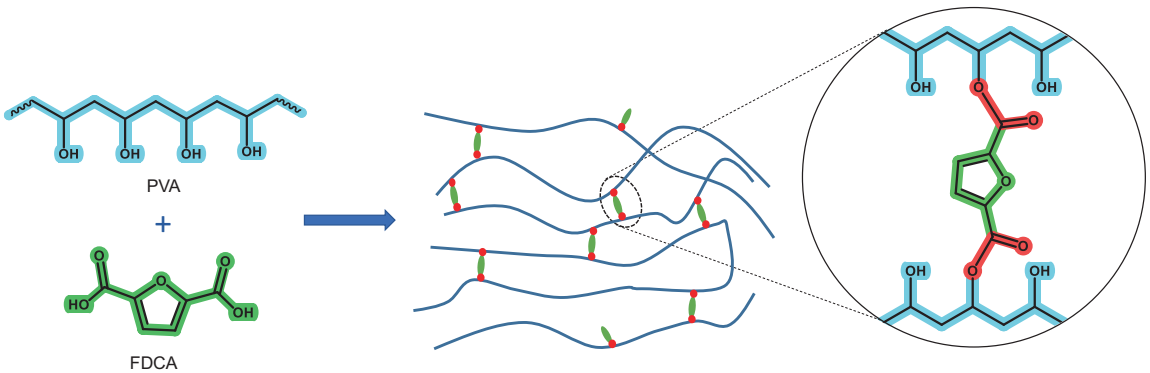

Fig. 2 Scheme of the crosslinking reaction between PVA and FDCA

machine with a load cell of 5 kN. The speed of the crosshead was 1 mm/min, and testing was conducted at 25 °C and 50% RH.

Results and discussion

Confirmation of the structure of the PVA-crosslink-FDCA films

The FTIR spectra of PVA and PVA-crosslink-FDCA 5% are shown in Fig. 3.

In the FTIR spectrum of PVA, an observed broad band ranging from 3200 to 3500 cm^{-1} was assigned to the stretching vibration of hydroxyl –OH groups. This finding indicates the existence of intra- and intermolecular hydrogen bonding among the –OH groups of the PVA chains. The stretching vibration of C_{sp3}–H bonds was recorded at 2932 cm^{-1}, including –CH and $–CH_2$ stretching of PVA. A peak at 1088 cm^{-1} was the C–O stretching vibration, while an absorption signal at 1655 cm^{-1} was attributed to carbonyl C=O stretching vibration. The slight absorption of C=O corresponded to residual acetate groups, which remained after the incomplete hydrolysis of poly(vinyl acetate) [12, 25, 27].

Similarly, these signals were also detected in the FTIR spectra of PVA-crosslink-FDCA 5% samples. However, a decrease in the intensity of the O–H signal was observed, and the maximum of this absorption band also shifted slightly toward shorter wavelengths (3305 cm^{-1} compared to 3272 cm^{-1} of PVA), indicating that the intensity of the hydrogen bonds between –OH groups was reduced. A sharp peak appearing at 3442 cm^{-1} could be due to the stretching vibration of –OH in the remaining unreacted carboxyl groups. In addition, the intensity of the characteristic signal of C=O groups at 1655 cm^{-1} increased in comparison to the corresponding signal of PVA. Thus, the changes in intensities and positions of the

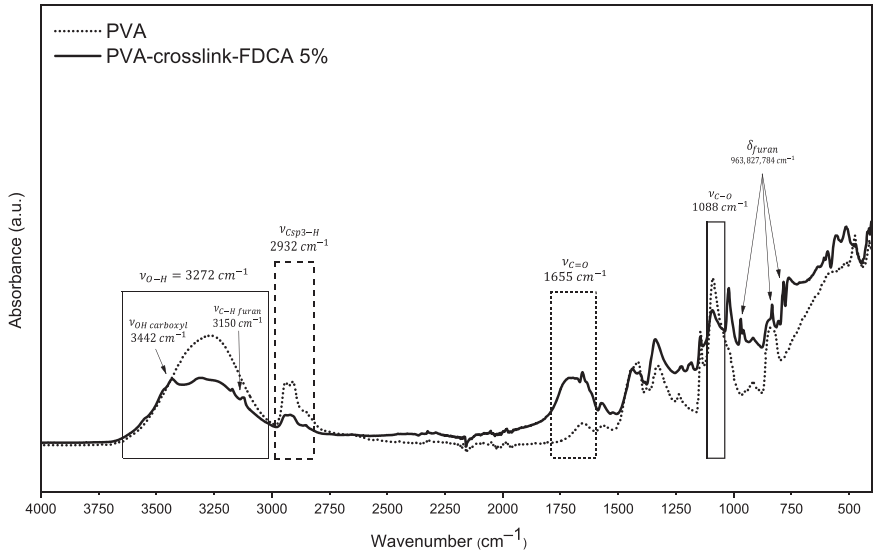

Fig. 3 ATR-FTIR spectra of PVA and PVA-crosslink-FDCA 5%

absorption signals of the O–H and C=O groups in the IR spectra confirmed the formation of ester crosslinks between the hydroxyl groups of PVA and carboxyl groups of FDCA. In addition, characteristic signals of furan rings were observed, such as C_{furan}–H vibration at approximately 2932 cm^{-1} and bending motions of furan at 963, 827, 784 cm^{-1}. These signals demonstrated the presence of furan rings in the modified materials.

At different concentrations of FDCA, the PVA-crosslink-FDCA samples exhibited noticeable variation in the IR spectra (Fig. 4). The spectrum for the 1% FDCA sample was identical to that for PVA. The absence of the sharp peak at approximately 3400 cm^{-1} indicated complete esterification. Meanwhile, a very broad band between 2300 and 3600 cm^{-1} was observed in the spectrum for the 10% FDCA sample. This absorption band was attributed to the absorption of carboxyl groups in the carboxylic acid dimers, which could be explained by the low solubility of FDCA in PVA [30]. At high concentrations, FDCA could aggregate to form its own phase and not participate in the crosslinking reaction. The existence of FCDA aggregates resulted in the appearance of a broad absorption band between 2300 and 3600 cm^{-1}.

The intensity ratios between the carbonyl band at 1655 cm^{-1} and the hydroxyl band at 3272 cm^{-1} increased with the FDCA concentrations in the crosslinked PVA samples. The ratio in PVA was 0.216. The ratios in PVA-crosslink-FDCA 1%, PVA-crosslink-FDCA 5%, and PVA-crosslink-FDCA 10% were 0.300, 1.088, and 5.500, respectively. Thus, this result also confirmed the formation of crosslinking ester bonds between the hydroxyl group of PVA and the carboxyl group of FDCA, as the number of –OH groups decreased and the number of C=O ester groups increased at higher FDCA concentrations [12, 14, 25, 26].

Swelling properties in water

Table 1 shows the SD in water for samples with different concentrations of FDCA and crosslinking times. Before crosslinking, the SD of the unmodified film was 98.46%. After 2 h of crosslinking, the SD decreased to 71.40% (1% FDCA), 52.10% (5% FDCA), and 35.57% (10% FDCA). In general, the SD decreased with increasing FDCA concentration.

The high tendency for swelling of PVA in water is linked to the large number of hydroxyl groups present and the mobility of the PVA chains. The hydroxyl groups easily form hydrogen bonds with water molecules, and the absorbed water molecules lead to the movements of polymer chains, causing an increase in dimensions and hence swelling of polymer films. Meanwhile, the mechanical properties also deteriorate. Crosslinking not only reduces the number of hydroxyl groups on PVA but also restricts the mobility of PVA chains relative to each other by covalently bonding them and hence restricts the absorption of water to fill in the space between PVA chains. In summary, crosslinking plays a dual role in controlling water absorption by limiting the movement of the PVA chains and by reducing the number of hydroxyl groups present.

On the other hand, from the swelling data, the crosslink density (n) of crosslinked PVA can be evaluated by using the Flory–Rehner equation [14, 27, 46]:

$$n = -\frac{\ln(1 - v_p) + v_p + \chi v_p^2}{V_o\left(v_p^{\frac{1}{3}} - \frac{v_p}{2}\right)} \quad (1)$$

where v_p is the volume fraction of the polymer in swollen mass, χ is the Flory–Huggins polymer-solvent

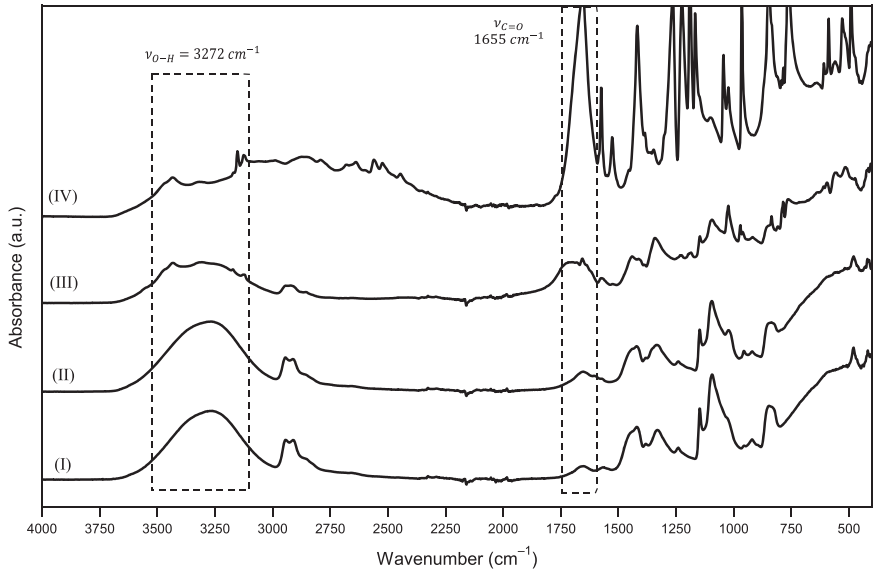

Fig. 4 ATR-FTIR spectra of (I) PVA and the prepared films, (II) PVA-crosslink-FDCA 1%, (III) 5%, and (IV) 10%

Table 1 Dependence of swelling degree and crosslink density on FDCA concentrations

FDCA concentration (%)	0	1	5	10
Swelling degree (%)	98.46 ± 1.84	71.40 ± 1.39	52.10 ± 3.70	35.57 ± 0.67
Crosslink density (10^{-3} mol/cm^3)		9.55	15.94	27.38

dimensionless interaction term (the value of χ is 0.49 taken from the literature for this PVA-water system [47]), and V_o is the molar volume of the solvent (18 ml/mol for water). v_p is related to the density of the solvent d_o (0.997 g/ml for water), the density of the polymer d_p (1.19 g/cm^3 for PVA), and the SD:

$$v_p = \frac{\frac{1}{d_p}}{\frac{SD}{d_o} + \frac{1}{d_p}} \quad (2)$$

The results of these calculations are presented in Table 1. Increasing FDCA concentrations were followed by a respective increase in the crosslink densities. Furthermore, the changes in SDs and crosslink densities with the variation of FDCA concentrations were also indications of the formation of ester crosslinks between PVA and FDCA.

Thermal properties

The thermal stability of PVA and the crosslinked PVA-FDCA films heat-treated at 120 °C for 2 h was analyzed using TGA measurements. TGA and derivative thermogravimetric (DTGA) curves are presented in Figs. 5 and 6.

The thermal decomposition of PVA occurs in three main stages [12, 14, 26]. The first stage occurring from 50 to 150 °C corresponds to the evaporation of bound and non-bound water molecules. In fact, the water content in PVA varies depending on several factors (humidity, temperature, and storage conditions), which can explain the absence in this region in the presented figures. The second intense peak at 267 °C was attributed to dehydration, the elimination of residual acetate groups, and chain scissions at these unhydrolyzed sites of PVA [48, 49]. The third decomposition step was observed with a maximum at 420 °C and was associated with chain scissions of polyenes and intramolecular cyclization [48, 49].

In the case of 1% and 5% FDCA concentrations, these three distinct degradation steps can be observed as well. In addition, there was an additional decomposition peak between the previously described second and third stages. This additional step was associated with the loss of most of the products' weights.

Similar to the degradation pattern of PVA, the first slight weight loss was observed between 100 and 200 °C due to the removal of water molecules. The peak in the 200–300 °C region corresponded to dehydration, deacetylation, and chain scissions. As crosslinking led to structures with a higher thermal stability in this range, chain scissions and the release of low-molecular-weight polyenes were observed to a lesser extent. The main decomposition of PVA-crosslink-FDCA occurred in the region of 300–400 °C. Thus, this decomposition stage was likely due to the cleavage of FDCA crosslinks [50] and C–C bonds of the main chains, which resulted in the conversion of most of the crosslinked polymer into gaseous products. Maximum decomposition for this stage was observed at higher temperatures for higher concentrations of FDCA (354 °C for 1% FDCA and 371 °C for 5% FDCA).

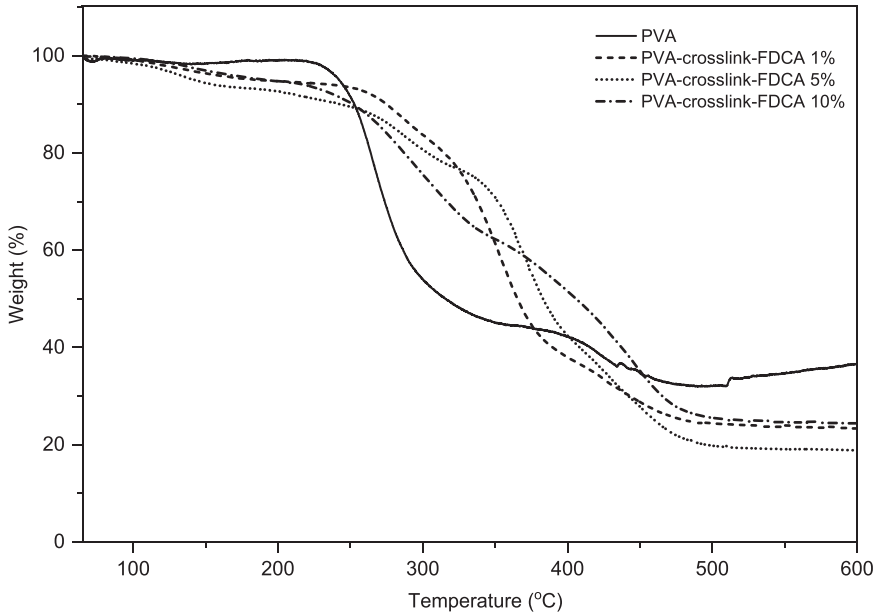

Fig. 5 TGA curves of PVA and PVA-crosslink-FDCA

The final step between 400 and 500 °C resulted from the complete decomposition of any remaining residues.

The decomposition pattern of PVA-crosslink-FDCA 10% differed from the other two concentrations. Hardly any additional degradation steps were observed when compared to PVA, and more weight was lost in the 200–350 °C regions when compared to the 1 and 5% FDCA samples. The higher density of crosslinks with very rigid FDCA molecules could lead to PVA chains being constrained in unstable conformations after crosslinking. These chains were then already susceptible to chain scission at the early stage of degradation, which generated free radicals and initiated further propagating chain cleavage. However, the decomposition maximum of the second stage shifted to a higher temperature than that of PVA; therefore, an improvement in the thermal stability of PVA was still observed in this case.

Mechanical properties

The mechanical properties, such as Young's modulus, stress at break, and elongation at break, were investigated at 25 °C and 50% RH. Typical strain–stress curves of PVA and crosslinked PVAs are shown in Fig. 7. In Table 2 and Fig. 7, we can see that the elongation at break of PVA and PVA-crosslink-FDCA was quite similar. This implies that crosslinking using FDCA concentrations lower than 10% does not exert a noticeable effect on the elongation at break of PVA. These samples also exhibited quite similar strain–stress behaviors, which were typical for ductile and tough plastics. On the other hand, Young's modulus of the PVA films increased with the addition of FDCA, thus implying that the stiffness of the samples increased. Similarly, at low FDCA concentrations (1% and 5%), the stress at break of PVA-crosslink-FDCA samples was found to significantly improve compared to that of PVA, which was attributed to the effect of crosslinks present in the sample. However, the response between the stresses at break and the higher FDCA concentration became somewhat less notable. There was no significant increase in tensile strength, and the strain–stress curves of the samples with 5 and 10% FDCA were identical. This finding is probably related to the tendency to form one-sided crosslinks and intramolecular crosslinks at high concentrations of dicarboxylic acid, which do not have a favorable correlation with the strength of crosslinked PVA [14]. In addition, FDCA aggregation due to low solubility in PVA (as previously discussed) reduced crosslinking efficiency. Overall, we confirm the efficiency of the crosslinking in the samples formed by FDCA, and the mechanical properties are in good agreement with the thermal properties.

Conclusion

The swelling behavior and thermal and mechanical properties of biodegradable PVA were successfully tuned by crosslinking with a biobased FDCA crosslinker. The SD of PVA decreased from 98 to 36% at an FDCA concentration of 10%. The thermal stability of PVA was improved significantly, especially at low FDCA concentrations of 1 and 5%, where degradation maximums occurred at 354 and 371 °C, respectively, compared to 267 °C for unmodified PVA. A twofold increase in tensile strength for the biodegradable PVA was achieved by

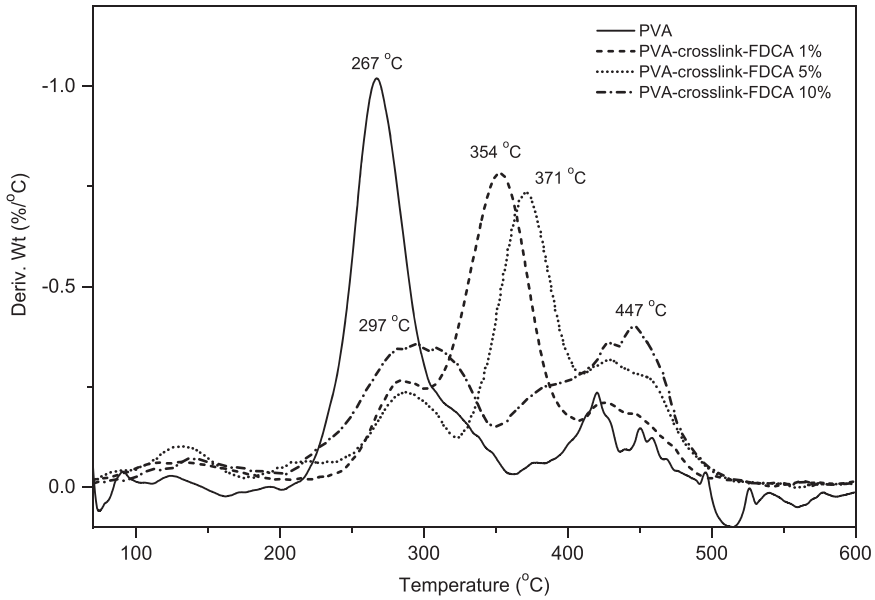

Fig. 6 DTGA curves of PVA and PVA-crosslink-FDCA

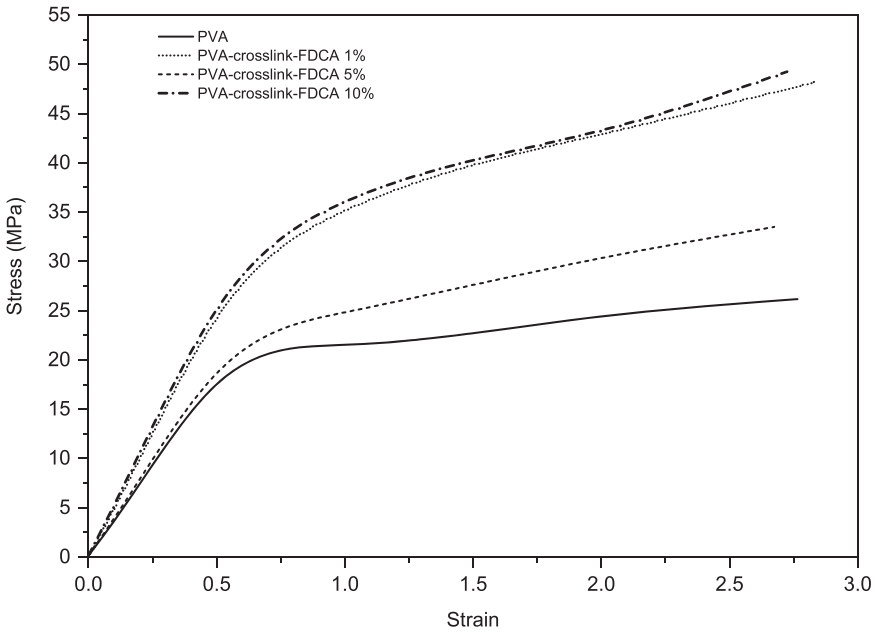

Fig. 7 Strain–stress curves of PVA and PVA-crosslink-FDCA

Table 2 Young's modulus, tensile strength, and elongation at break of PVA and crosslinked PVA with various concentrations of FDCA at 1, 5, and 10%

Sample	Elongation at break (%)	Young's modulus (MPa)	Tensile strength (MPa)
PVA	273 ± 31	352 ± 15	25.5 ± 1.2
PVA-crosslink-FDCA 1%	268 ± 22	377 ± 24	33.0 ± 0.5
PVA-crosslink-FDCA 5%	282 ± 35	483 ± 27	48.2 ± 2.6
PVA-crosslink-FDCA 10%	275 ± 16	505 ± 18	49.1 ± 3.1

crosslinking with 5% FDCA. In addition, the elongation at break remained constant compared to that of PVA. A higher concentration of FDCA did not result in further improvements in either the thermal or mechanical properties. Furthermore, lower concentrations of the crosslinker are also expected to be beneficial in terms of the biodegradation of PVA since a high crosslink density distorts both the microstructure and morphology of the polymer. In conclusion, we demonstrated that FDCA can be a potential biobased crosslinking agent for PVA in an attempt to improve the thermomechanical properties of this biodegradable polymer.

Acknowledgements This research is funded by the Vietnam National Foundation for Science and Technology Development (NAFOSTED) under grant number 104.02-2019.12. The authors are grateful to Nigel Van de Velde for the valuable comments and corrections during the revision of the manuscript.

Compliance with Ethical Standard

Conflict of interest The authors declare no competing interests.

Publisher's note Springer Nature remains neutral with regard to jurisdictional claims in published maps and institutional affiliations.

References

1. Muthuraj R, Misra M, Mohanty AK. Biodegradable compatibilized polymer blends for packaging applications: a literature review. J Appl Polym Sci. 2018;135:45726.
2. Scaffaro R, Maio A, Sutera F, Gulino EF, Morreale M. Degradation and recycling of films based on biodegradable polymers: a short review. Polymers. 2019;11:651.
3. Jayanth D, Kumar PS, Nayak GC, Kumar JS, Pal SK, Rajasekar R. A review on biodegradable polymeric materials striving towards the attainment of green environment. J Polym Environ. 2018;26:838–65.
4. Narancic T, O'Connor KE. Plastic waste as a global challenge: are biodegradable plastics the answer to the plastic waste problem? Microbiology. 2019;165:129–37.
5. Shen M, Song B, Zeng G, Zhang Y, Huang W, Wen X, et al. Are biodegradable plastics a promising solution to solve the global plastic pollution? Environ Pollut. 2020;263:114469.
6. Manfra L, Marengo V, Libralato G, Costantini M, De Falco F, Cocca M, et al. Biodegradable polymers: a real opportunity to solve marine plastic pollution? J Hazard Mater. 2021;416:125763.
7. Halima NB. Poly (vinyl alcohol): review of its promising applications and insights into biodegradation. RSC Adv. 2016;6:39823–32.
8. Aslam M, Kalyar MA, Raza ZA. Polyvinyl alcohol: a review of research status and use of polyvinyl alcohol based nanocomposites. Polym Eng Sci. 2018;58:2119–32.
9. Feldman D. Poly (vinyl alcohol) recent contributions to engineering and medicine. J Compos Sci. 2020;4:175.
10. Shimao M. Biodegradation of plastics. Curr Opin Biotechnol. 2001;12:242–7.
11. Kawai F, Hu X. Biochemistry of microbial polyvinyl alcohol degradation. Appl Microbiol Biotechnol. 2009;84:227–37.
12. Sonker AK, Tiwari N, Nagarale RK, Verma V. Synergistic effect of cellulose nanowhiskers reinforcement and dicarboxylic acids crosslinking towards polyvinyl alcohol properties. J Polym Sci Part A: Polym Chem. 2016;54:2515–25.
13. Falqi FH, Bin-Dahman OA, Hussain M, Al-Harthi MA. Preparation of miscible PVA/PEG blends and effect of graphene concentration on thermal, crystallization, morphological, and mechanical properties of PVA/PEG (10 wt%) blend. Int J Polym Sci. 2018;2018:8527693.
14. Sonker AK, Rathore K, Nagarale RK, Verma V. Crosslinking of polyvinyl alcohol (PVA) and effect of crosslinker shape (aliphatic and aromatic) thereof. J Polym Environ. 2018;26:1782–94.
15. Kim K-J, Lee S-B, Han N-W. Kinetics of crosslinking reaction of PVA membrane with glutaraldehyde. Korean J Chem Eng. 1994;11:41–47.
16. Figueiredo KCS, Alves TLM, Borges CP. Poly (vinyl alcohol) films crosslinked by glutaraldehyde under mild conditions. J Appl Polym Sci. 2009;111:3074–80.
17. Liu L, Kentish SE. Pervaporation performance of crosslinked PVA membranes in the vicinity of the glass transition temperature. J Membr Sci. 2018;553:63–69.
18. Ji W, Afsar NU, Wu B, Sheng F, Shehzad MA, Ge L, et al. In-situ crosslinked SPPO/PVA composite membranes for alkali recovery via diffusion dialysis. J Membr Sci. 2019;590:117267.
19. Zhang Y, Zhu PC, Edgren D. Crosslinking reaction of poly (vinyl alcohol) with glyoxal. J Polym Res. 2010;17:725–30.
20. Leone G, Consumi M, Pepi S, Pardini A, Bonechi C, Tamasi G, et al. Poly-vinyl alcohol (PVA) crosslinked by trisodium trimetaphosphate (STMP) and sodium hexametaphosphate (SHMP): effect of molecular weight, pH and phosphorylating agent on length of spacing arms, crosslinking density and water interaction. J Mol Struct. 2020;1202:127264.
21. Miyazaki T, Takeda Y, Akane S, Itou T, Hoshiko A, En K. Role of boric acid for a poly (vinyl alcohol) film as a cross-linking agent: Melting behaviors of the films with boric acid. Polymer. 2010;51:5539–49.
22. Bolto B, Tran T, Hoang M, Xie Z. Crosslinked poly (vinyl alcohol) membranes. Prog Polym Sci. 2009;34:969–81.
23. Heydari M, Moheb A, Ghiaci M, Masoomi M. Effect of crosslinking time on the thermal and mechanical properties and pervaporation performance of poly (vinyl alcohol) membrane crosslinked with fumaric acid used for dehydration of isopropanol. J Appl Polym Sci. 2013;128:1640–51.
24. Jose J, Al-Harthi MA. Citric acid crosslinking of poly (vinyl alcohol)/starch/graphene nanocomposites for superior properties. Iran Polym J. 2017;26:579–87.
25. Sonker AK, Teotia AK, Kumar A, Nagarale RK, Verma V. Development of polyvinyl alcohol based high strength biocompatible composite films. Macromol Chem Phys. 2017;218:1700130.
26. Sonker AK, Rathore K, Teotia AK, Kumar A, Verma V. Rapid synthesis of high strength cellulose–poly (vinyl alcohol)(PVA) biocompatible composite films via microwave crosslinking. J Appl Polym Sci. 2019;136:47393.
27. Sonker AK, Verma V. Influence of crosslinking methods toward poly (vinyl alcohol) properties: microwave irradiation and conventional heating. J Appl Polym Sci. 2018;135:46125.
28. Kudoh Y, Kojima T, Abe M, Oota M, Yamamoto T. Proton conducting membranes consisting of poly (vinyl alcohol) and poly (styrene sulfonic acid): crosslinking of poly (vinyl alcohol) with and without succinic acid. Solid State Ion. 2013;253:189–94.
29. Dlamini DS, Wang J, Mishra AK, Mamba BB, Hoek EMV. Effect of cross-linking agent chemistry and coating conditions on physical, chemical, and separation properties of PVA-Psf composite membranes. Sep Sci Technol. 2014;49:22–29.
30. Salgado-Chavarría D, Palacios-Alquisira J. Poly (vinyl alcohol) membranes cross-linked with maleic anhydride and 2, 5-furandicarboxylic acid: conventional heating and microwave irradiation. ChemistrySelect. 2020;5:4826–38.
31. Sajid M, Zhao X, Liu D. Production of 2, 5-furandicarboxylic acid (FDCA) from 5-hydroxymethylfurfural (HMF): recent progress focusing on the chemical-catalytic routes. Green Chem. 2018;20:5427–53.
32. Liguori F, Barbaro P, Calisi N. Continuous-flow oxidation of HMF to FDCA by resin-supported platinum catalysts in neat water. ChemSusChem. 2019;12:2558–63.
33. Liu X, Zhang M, Li Z. CoO x-MC (MC= mesoporous carbon) for highly efficient oxidation of 5-hydroxymethylfurfural (5-HMF) to 2,5-furandicarboxylic acid (FDCA). ACS Sustain Chem Eng. 2020;8:4801–8.
34. Guan W, Zhang Y, Chen Y, Wu J, Cao Y, Wei Y, et al. Hierarchical porous bowl-like nitrogen-doped carbon supported bimetallic AuPd nanoparticles as nanoreactors for high efficient catalytic oxidation of HMF to FDCA. J Catal. 2021;396:40–53.

35. Menegazzo F, Ghedini E, Signoretto M. 5-Hydroxymethylfurfural (HMF) production from real biomasses. Molecules. 2018;23:2201.
36. Sonsiam C, Kaewchada A, Jaree A. Synthesis of 5-hydroxymethylfurfural (5-HMF) from fructose over cation exchange resin in a continuous flow reactor. Chem Eng Process. 2019;138:65–72.
37. Zhang Y, Li B, Guan W, Wei Y, Yan C, Meng M, et al. One-pot synthesis of HMF from carbohydrates over acid-base bi-functional carbonaceous catalyst supported on halloysite nanotubes. Cellulose. 2020;27:3037–54.
38. El Fergani M, Candu N, Tudorache M, Bucur C, Djelal N, Granger P, et al. From useless humins by-product to Nb@graphite-like carbon catalysts highly efficient in HMF synthesis. Appl Catal A: Gen. 2021;618:118130.
39. Fei X, Wang J, Zhu J, Wang X, Liu X. Biobased poly (ethylene 2, 5-furancoate): No longer an alternative, but an irreplaceable polyester in the polymer industry. ACS Sustain Chem Eng. 2020;8:8471–85.
40. Terzopoulou Z, Papadopoulos L, Zamboulis A, Papageorgiou DG, Papageorgiou GZ, Bikiaris DN. Tuning the properties of furandicarboxylic acid-based polyesters with copolymerization: a review. Polymers. 2020;12:1209.
41. Trung NV, Nguyen MN, Ngoc ANT, Thi NP, Quang TT, Thi TT. Synthesis and characterizations of biobased copolymer poly (ethylene-co-butylene 2, 5-furandicarboxylate). Int J Polym Sci. 2021;2021:9104546.
42. Zhang D, Dumont MJ. Advances in polymer precursors and bio-based polymers synthesized from 5-hydroxymethylfurfural. J Polym Sci Part A: Polym Chem. 2017;55:1478–92.
43. Burgess SK, Karvan O, Johnson JR, Kriegel RM, Koros WJ. Oxygen sorption and transport in amorphous poly (ethylene furanoate). Polymer. 2014;55:4748–56.
44. Burgess SK, Mikkilineni DS, Daniel BY, Kim DJ, Mubarak CR, Kriegel RM, et al. Water sorption in poly (ethylene furanoate) compared to poly (ethylene terephthalate). Part 1: equilibrium sorption. Polymer. 2014;55:6861–9.
45. Burgess SK, Mikkilineni DS, Daniel BY, Kim DJ, Mubarak CR, Kriegel RM, et al. Water sorption in poly (ethylene furanoate) compared to poly (ethylene terephthalate). Part 2: kinetic sorption. Polymer. 2014;55:6870–82.
46. Rimdusit N, Jubsilp C, Mora P, Hemvichian K, Thuy TT, Karagiannidis P, et al. Radiation graft-copolymerization of ultrafine fully vulcanized powdered natural rubber: effects of styrene and acrylonitrile contents on thermal stability. Polymers. 2021;13:3447.
47. Yang M-H, Chu T-J. The determination of interaction parameter $\chi 1$ for polyvinyl alcohol and water from the diffusion data. Polym Test. 1993;12:57–64.
48. Peng Z, Kong LX. A thermal degradation mechanism of polyvinyl alcohol/silica nanocomposites. Polym Degrad Stab. 2007;92:1061–71.
49. Gilman JW, VanderHart Dl, Kashiwagi T. Thermal decomposition chemistry of poly(vinyl alcohol). In Fire and polymers II, 599. ACS Symposium Series. American Chemical Society; 1995. p. 161–85.
50. Tsanaktsis V, Vouvoudi E, Papageorgiou GZ, Papageorgiou DG, Chrissafis K, Bikiaris DN. Thermal degradation kinetics and decomposition mechanism of polyesters based on 2,5-furandicarboxylic acid and low molecular weight aliphatic diols. J Anal Appl Pyrolysis. 2015;112:369–78.